Journal of the European Ceramic Society 20 (2000) 347–355

Multifunctional Si_3N_4/(β-SiAlON + TiN) layered composites

Zoltán Lenčéš [a,*], Pavol Šajgalík [b], Motohiro Toriyama [c], Manuel E. Brito [c], Shuzo Kanzaki [c]

[a] *Synergy Ceramics Laboratory, Fine Ceramics Research Association, Nagoya 462-8510, Japan*
[b] *Institute of Inorganic Chemistry, Slovak Academy of Sciences, 842 36 Bratislava, Slovakia*
[c] *National Industrial Research Institute of Nagoya, Nagoya 462-8510, Japan*

Received 10 March 1999; received in revised form 15 June 1999; accepted 28 June 1999

Abstract

Layered multifunctional ceramic composites on the base of Si_3N_4 and TiN have been prepared by tape casting. The reaction conditions for in situ preparation of β-SiAlON + TiN composite were optimised and dense Si_3N_4/(β-SiAlON + TiN) layered materials were prepared by hot pressing. The bending strength and fracture toughness of layered materials measured in the direction perpendicular to the layer alignment were remarkably higher (1184 MPa and 9.75 MPa $m^{1/2}$) in comparison to the "monolithic" β-SiAlON + TiN composite (647 MPa and 4.71 MPa $m^{1/2}$). High anisotropy was achieved for the electrical resistance of the layered materials in parallel (6.10^{-2} Ω cm) and perpendicular (5×10^{11} Ω cm) direction to the layer alignment.

Keywords: Composites; Electrical properties; Layered composites; Mechanical properties; Si_3N_4; Tape casting; TiN

1. Introduction

Design of ceramic composites with layered structure has recently gained increasing attention because layered ceramic materials show decreased sensitivity to defects and they display a balanced combination of engineering properties.[1,2] The mechanical properties of layered materials are dependent on the stress status of individual layers. The character of residual stresses, i.e. compressive or tensile, are a consequence of different physical constants of individual layers, e.g. thermal expansion coefficient and Young's modulus. Additionally, the stress status of certain layer can be modified by the layer thickness, sinterability of the powder and used sintering method.[3–5] Layered ceramic materials pay for the increased quality by loosing isotropy of their mechanical and physical properties. However, several structural applications require anisotropic properties; for instance, different thermal or electrical conductivity in parallel and perpendicular direction to the layers.

Bearing the above in mind, the preparation of Si_3N_4/(β-SiAlON + TiN) layered composites with anisotropic properties was carried out. All the components of this composite are potential candidates for special engineering applications, such as cutting tools, structural parts of combustion engines, etc. Their advantageous properties are combined in this case through layered design: Si_3N_4 layers with high strength and (β-SiAlON + TiN) layers with higher hardness and low thermal conductivity. Moreover, the β-SiAlON ($Si_{6-z}Al_zO_zN_{8-z}$, where $0 < z < 4.2$) matrix has a good oxidation resistance,[6] and the dispersed TiN comparable higher electrical conductivity. Remarkable anisotropy in electrical conductivity is expected, because Si_3N_4 is an insulator with extremely high electrical resistivity 10^{13} Ω cm, while TiN is an electroconductive material with electrical resistivity of 3.3×10^{-5} Ω cm.[7] Addition of 20–40 vol% TiN in Si_3N_4 matrix could result in good electrical conductivity.[8–12]

Si_3N_4/TiN electroconductive composites have been fabricated by sintering or hot-pressing of TiN and Si_3N_4 powder mixture with different sintering additives,[7,8,13–15] by nitridation of Si powder compact containing TiN particles[9] or by direct nitridation of silicon and titanium, using SHS process.[16] From the economical point of view an interesting route is the preparation of TiN by in situ reduction of TiO_2 in the Si_3N_4 matrix.[17,18] The

* Corresponding author at present adress: Institute of Inorganic Chemistry, SAS, Dubravska cesta 9, SK-842 36 Bratislava, Slovakia.

0955-2219/00/$ - see front matter
PII: S0955-2219(99)00172-7

electrical properties of this composite were better in comparison to materials with direct addition of the same amount of TiN particles due to the good, network-like distribution of fine TiN particles. By direct nitridation of Si + TiO_2 powder mixture and subsequent hot-pressing of sintering additives containing sample Si_2N_2O/TiN composite has also been prepared.[11] Oxidation resistant electroconductive SiAlON/TiN ceramic composites were prepared either by the addition of TiN particles to SiAlON powder mixture,[19] or by direct nitridation of Si + Al + TiO_2 powder mixture.[20]

As can be seen from the brief review, high attention is devoted to the preparation of Si_3N_4/TiN based composites by different routes. Except of particulate composites also laminated ceramics of the same phase composition are investigated. Improved damage resistant Si_3N_4/TiN trilayer composites have been already reported.[21,22]

Present paper deals with the optimisation of reaction conditions for the in situ preparation of β-SiAlON/TiN composite with the aim to get a fully dense composite. The ambition of the paper is to design the Si_3N_4/β-SiAlON + TiN) layered composite with enhanced mechanical properties and modified electrical and thermal properties. The role of the residual stresses with respect to the mechanical properties will be also discussed.

2. Experimental procedure

Two kinds of ceramic sheets on the base of Si_3N_4 and β-SiAlON/TiN composite were prepared by tape casting. The sheets are designated as SN and SNT, respectively. The starting powder mixture of SN sheets consisted of commercial α-Si_3N_4 powder (E-10, Ube Industries, Japan), 5 wt% Y_2O_3 (27 m^2/g, Hokko Chem., Japan) and 2 wt% Al_2O_3 (173 m^2/g, Hokko Chem., Japan) sintering additives. The powders were ball-milled in Si_3N_4 pot for 2 h. Toluene and *n*-butanol, 4:1 in volume ratio was the solvent, which contained 3 wt% dispersant (Diamine RRT, Kao Chemicals, Japan). After ball milling 9 wt% Polyvinyl-butiral resin (BM-S grade, Sekisui Chemicals, Japan) and 2.25 wt% dioctyl adipate plasticizer (Wako Pure Chemical Industries, Japan) were added. Into two SN batches also 2 or 5 vol% β-Si_3N_4 seeds (produced in our lab.[23]) were dispersed. The suspension was homogenised for 35 h in Nylon pot with light balls to avoid the breaking of elongated seeds. Green sheets were formed from the slurries by tape casting with final thickness of 100–110 μm. The Si_3N_4 tapes are abbreviated as SN0 (without seeds), SN2 (2 vol% seeds) and SN5 (5 vol% seeds).

The SNT sheets were prepared by the same processing and consisted of α-Si_3N_4, Al_2O_3, AlN (type F, Tokuyama Co., Japan) and TiO_2 (<5 μm, Wako Pure Chemical Industries, Japan). The composition was adjusted to have 10 and 20 vol% TiN in the final product after the following reactions:

$$3\ TiO_2 + 4\ AlN = 3\ TiN + 2\ Al_2O_3 + \frac{1}{2}N_2 \quad (1)$$

$$(6-z)\ Si_3N_4 + z\ (Al_2O_3 + AlN) = 3\ Si_{6-z}Al_zO_zN_{8-z} \quad (2)$$

which can be summarised as:

$$4(6-z)\ Si_3N_4 + 6z\ TiO_2 + 12z\ AlN = 12\ Si_{6-z}Al_zO_zN_{8-z} + 6z\ TiN + zN_2 \quad (3)$$

While TiN remains as an inert phase in the product, Al_2O_3 from reaction (l) is incorporated to the β-SiAlON according to reaction (Eq. 2). The theoretical value of z is about 1.7 and 3.9 in the formula $Si_{6-z}Al_zO_zN_{8-z}$. It should be mentioned that the summarised reaction (Eq. 3) consists of two steps, because reaction (Eq. 1) proceeds in the temperature range of 1300–1500°C, while reaction (Eq. 2) above this temperature, depending on the impurity (mainly SiO_2) content.

The SNT tapes were covered from one side with BN spots by screen coating. The BN slurry contained 13 wt% Y_2O_3 and Al_2O_3 as sintering additives. The diameter of BN spots was 250 μm and the distance among them about 150 μm (Fig. 1)

The ceramic sheets were stacked after punching to each other by warm pressing at 120°C for 20 min. Two kinds of layer sequences were produced, where two (L2*hk*) or four (L4*hk*) different layers were alternated and are depicted in Fig. 2a and b with the proposed crack propagation. The *h* variable in the sample designation shows

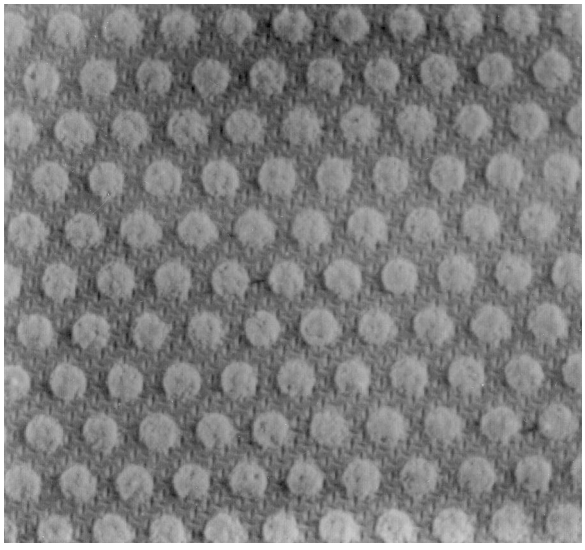

Fig. 1. Screen-coated BN spots on the SNT green sheet. The diameter of BN spots is 250 μm.

the heat treatment (see below) and k expresses the TiN content in tens of vol%. The main sample characteristics are listed in Table 1. The binder was removed from the green samples under N_2 + 5% H_2 flow at 600°C for 3 hours and subsequently at 450°C for 3 hours under dry air. Because of slight delamination during annealing, the samples were CIP-ed at 250 MPa pressure. Samples were sintered in a hot pressing graphite resistance furnace. Up to 1370°C the same heating-rate 10°C/min was used for all samples. From this temperature three different heat treatment schedules (A, B and C) were used to find out the optimum reaction conditions for *in situ* preparation of TiN:

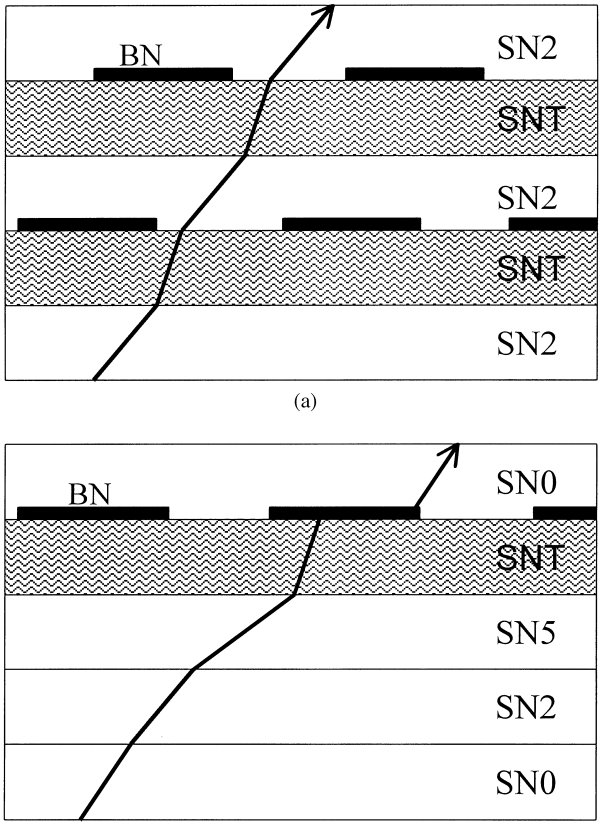

Fig. 2. Schematic of layer sequences and proposed crack propagation: (a) L2*hk* samples with two alternating layers, (b) L4*hk* samples with four alternating layers. SN0 = Si_3N_4 without seeds, SN2 = Si_3N_4 + 2 vol% seeds, SN5 = Si_3N_4 + 5 vol% seeds, SNT = β-SiAlON + TiN.

Table 1
Sample characteristics

Sample	Structure	Layers[a]	Heat treatment	TiN (vol%)
MB1	Monolithic	1	B	10
L2B1	Layered	2	B	10
L4A1	Layered	4	A	10
L4B1	Layered	4	B	10
L4B2	Layered	4	B	20

[a] Number of layers in layer units, which are repeated several times.

A. holding time at 1370°C for 1 h under vacuum
B. 2°C/min up to 1500°C under vacuum
C. 2°C/min up to 1600°C under vacuum

Mechanical load was not applied in this stage. After vacuum heat treatment in all cases nitrogen gas was introduced and continuously increasing mechanical load was applied. The final hot pressing conditions at 1820°C for 3 h were 0.4 MPa nitrogen atmosphere and 30 MPa load-pressure.

Bulk densities were measured by the Archimedes method in water. The composition of β-SiAlON was determined by X-ray diffraction. The diffraction patterns were collected on the powdered samples with primary beam monochromatized Co$K_{\alpha 1}$ radiation using a STOE Stadi P transmission diffractometer configured with a linear position sensitive detector. The microstructure was characterised by Scanning Electron Microscopy (SEM) on polished and plasma etched (CF_4 + 10% O_2) surfaces. Three-point flexural strength measurements were carried out on 3×4×36 mm samples with a span of 30 mm, and a cross-head speed of 0.5 mm/min at room temperature. The fracture toughness was measured by single-edge-V-notched beam (SEVNB) method with a V notch root radius of 18 μm. The thermal conductivity was measured by laser flash method using a thermal constant analyser (TC-3000, Shinku-Riko, Japan) on circular specimens 2 mm thick and sputter-coated with gold film to prevent direct transmission of the laser. Carbon layer was deposited on both sides of specimens to enhance the absorption of the laser beam. The electrical conductivity was measured by direct contact measurement method.

3. Results and Discussion

3.1. Reaction conditions

The density measurements and SEM observations showed remaining porosity (about 3–5%) in samples sintered under reaction conditions A, while the samples sintered under conditions B and C were fully dense. The pores were not eliminated in the former samples, because the load was applied before reaction (Eq. 1) was completely finished. Removal of gaseous reaction product (N_2) at higher temperatures was more difficult due to the partly closed porosity of outer shell and consequently in the sintered body relatively large localised pores with diameter up to 50 μm were found. Samples prepared under conditions B and C had a similar microstructure and due to better economic efficiency, reaction schedule B was selected for the sintering of all samples which were used for mechanical tests, except the L4A1 sample. This layered sample was sintered under condition A to find out the influence of remaining

porosity on strength and also the flaw tolerance of layered sample.

3.2. Microstructure and mechanical properties

The side view of sintered, polished and plasma etched L2B1 and L4B1 samples with layered structure is shown in Fig. 3. The dark grey layers are Si_3N_4 and the light one (β-SiAlON + TiN) composites. The L2B1 sample consists of alternating (β-SiAlON + TiN) and Si_3N_4 layers (Figs. 2a and 3a). The structure of L4B1 layered sample is more complex (Fig. 3b) and it is built from three different Si_3N_4 layers with increasing seed content, i.e. 0, 2 and 5 vol% towards the (β-SiAlON + TiN) layer, as it is schematically shown in Fig. 2b. The aim of this design was to get gradually increasing compressive internal stresses in the layers after sintering. In our previous work it was shown that the strength of layered composite can be expressed by the equation:[24]

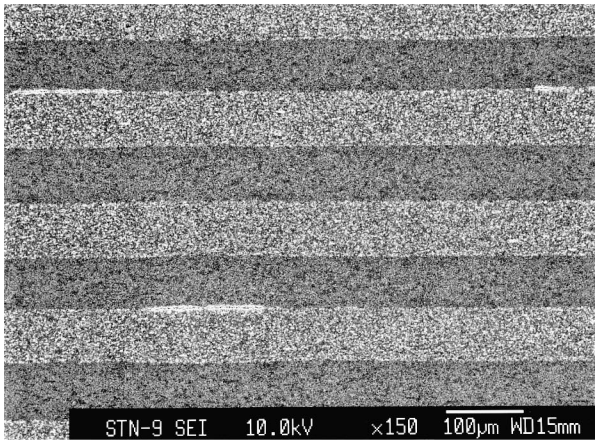

(a)

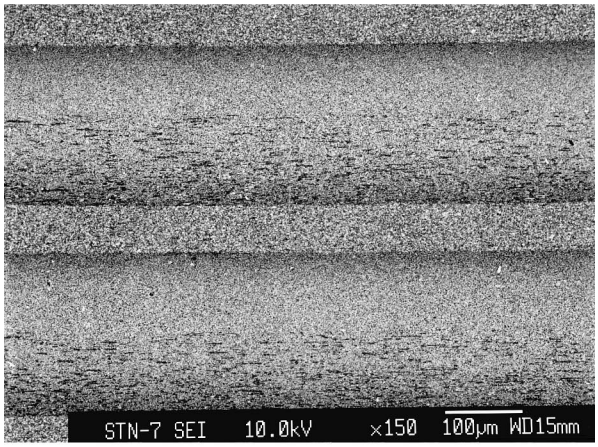

(b)

Fig. 3. SEM micrographs of polished and plasma etched surface of layered (a) L2B1 and (b) L4B1 samples.

$$\sigma = \sum_{i=1}^{n} V_i \sigma_i + \sum_{j=1}^{n-1} \Delta\sigma_j \tag{4}$$

where σ_i is the strength of monoliths which the layered composite consists of, V_i is their volume fraction ($\sum_{i=1}^{n} V_i = 1$) and $\Delta\sigma_j$ is the difference in stress status of adjacent layers. The difference of internal stresses in symmetrical three layered composite is defined by the following equation:[3]

$$\Delta\sigma = \frac{E_1 E_2(\alpha_2 - \alpha_1)(d_2 + 2d_1)\Delta T}{(1 - v_1)E_2 d_2 + 2(1 - v_2)E_1 d_1} \tag{5}$$

where v is the Poisson's ratio, E the Young's modulus, d the layer thickness, $\Delta T = T_j - T_o$, the difference between temperature of rigid joints formation between the layers (T_j) and room temperature (T_o), α_1 and α_2 parameters include the coefficients of thermal expansion (CTE) and shrinkage of adjacent layers. Eq. (5) and our previous results of model experiments[25] were the base for the design of layered material (Fig. 2b). If the contribution of layer interface between two layers to the total strength should be positive, also the sign of $\Delta\sigma$ must be positive, i.e. the next layer is under compression. In case the layered composite consists of 40–60 layers, in practice it is difficult to fulfil the condition to have gradually increasing residual stresses across the whole sample. This condition was partly fulfilled in layered L4*hk* samples, although only for the layer unit, as is depicted in Fig. 2b. The last layer in the layer unit containing TiN (SNT layer) was under tension due to the higher CTE of TiN (9.4×10^{-6} K^{-1}) in comparison to Si_3N_4 (3.2×10^{-6} K^{-1}). This layer sequence was repeated several times across the sample.

According to Eq. (5), in case the particular layers consist of two different materials, e.g. Si_3N_4 and TiN, the residual stress will be higher in comparison to layers which differs only in microstructure of the same material, e.g. Si_3N_4. In the former case all the parameters (α, E, v, d) can be varied, while in the later one E and v are the same and only the layer thickness d and parameter α_i can be changed. In this work also d was kept almost constant for the Si_3N_4 layers and only the influence of α_i was studied. As it was mentioned, this parameter includes the CTE and shrinkage of layer. It is well known that the shrinkage of material prepared from fine powder is higher in comparison to coarser one due to the lower green density. Layers containing higher amount of seed particles were coarser (SN2, SN5 in Fig. 4) and the shrinkage decreased with increasing seed content. Also the alignment of small elongated grains grown on the β-Si_3N_4 nuclei present in the starting α-Si_3N_4 powder (about 3%) in the layer with fine microstructure is lower in comparison to the layers with big elongated grains grown on the seed particles (2 or 5

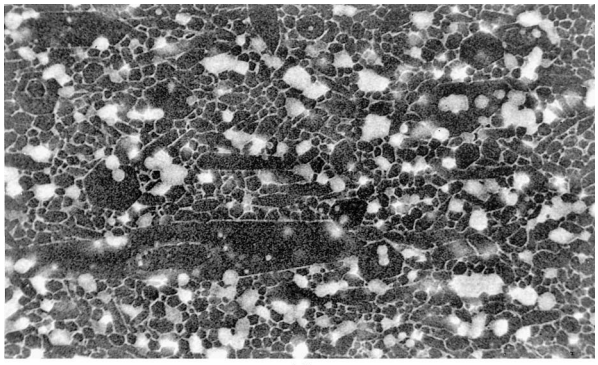

(a)

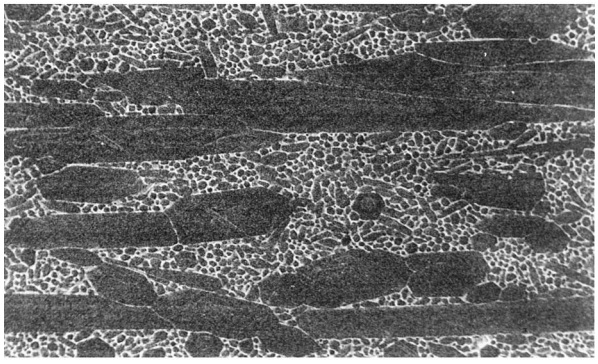

(b)

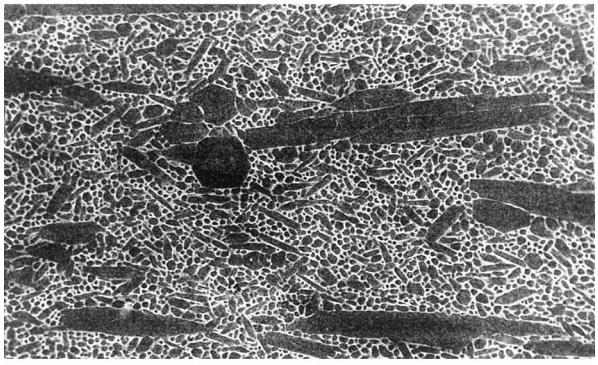

(c)

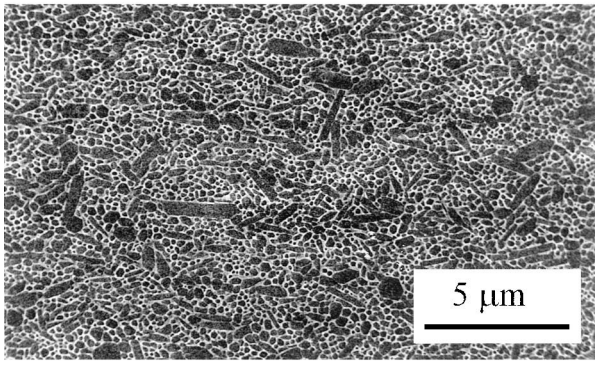

(d)

Fig. 4. SEM micrographs of individual plasma etched layers: (a) β-SiAlON + TiN, (b) Si_3N_4 + 5 vol% seeds, (c) Si_3N_4 + 2 vol% seeds, (d) Si_3N_4 without seeds.

vol%, respectively). The big elongated particles improved the alignment of small rod-like grains during hot pressing. The residual stress due to different shrinkage and oriented microstructure of adjacent layers composed of the same material (i.e. Si_3N_4) can be high enough to deflect the propagating crack[22] and the presence of different material inclusions is not necessary.[24] Taking into account the thermal expansion anisotropy of β-Si_3N_4 in *a* and *c* direction, where $\alpha_a = 3.3\times10^{-6}$ K^{-1} and $\alpha_c = 3.8\times10^{-6}$ K^{-1},[26] the stress status of adjacent Si_3N_4 layers can be partly influenced also by the amount of elongated Si_3N_4 particles, if they are preferentially oriented. This condition was fulfilled in the layered samples, because the ceramic green sheets were prepared by tape casting, what markedly increased the alignment of β-Si_3N_4 seed particles. Moreover, the samples were sintered by hot pressing and this technique itself introduced some residual stress anisotropy into the samples. The conservation of the stress anisotropy in the hot pressed samples can be explained by the oriented growth of the β-Si_3N_4 grains under pressure. Not only the seed particles, but also the longer in situ grown β-Si_3N_4 grains are oriented with the *c*-axis under an angle $>45°$ to the applied pressure. If the majority of grains is aligned nearly perpendicular to the hot pressing direction, like it is in the seeded Si_3N_4 layers, the compressive stresses in this direction will occur. The crack deflection on the layer interface between layers with 5 vol% seeds and (β-SiAlON + TiN) layer is shown in Fig. 5 Comparing about 20 cracks crossing different layer interfaces the crack deflections were more remarkable at this interface. The reason for this is that the residual stress was higher in adjacent Si_3N_4 and (β-SiAlON + TiN) layers in comparison to Si_3N_4 layers with different seed content. Si_3N_4 layers are under compression in a neighbourhood

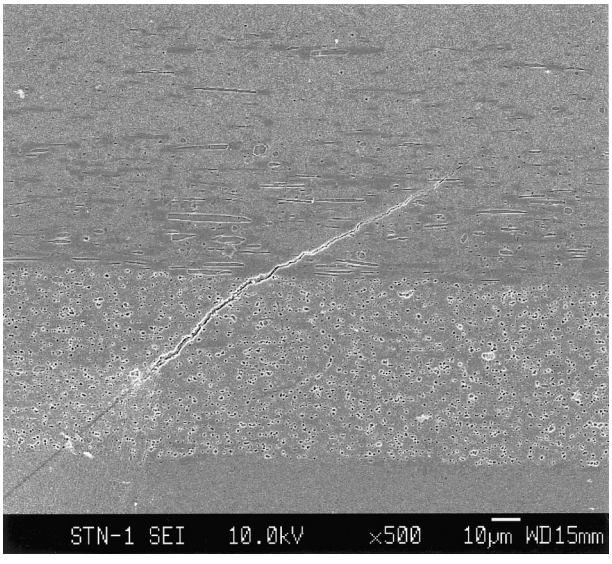

Fig. 5. Crack deflection at the layer interface.

of TiN containing layers due to the higher CTE of TiN. The composite (β-SiAlON + TiN) layers are under tension. To avoid the cracking of this layer due to the large stress differences, the TiN content was adjusted to 10 and 20 vol%, because in our previous results with ~25 vol% TiN spontaneous cracking of the outer layer in normal direction to the interface was observed.[22] Moreover, in recent case the (β-SiAlON + TiN) layer was also covered with BN spots from one side, what allowed a limited slip on layer interface and partial release of tensile stresses. The diameter of BN spots was 250 μm and their distance from each other 150 μm, which resulted in a total area of 26% BN on the ceramic sheet. The consequence was a stress anisotropy on both sides of (β-SiAlON + TiN) layer. The compressive stress in the Si_3N_4 layer strongly bonded to (β-SiAlON + TiN) layer was higher in comparison to the Si_3N_4 layer from another side, which was detached by BN spots. These layer sequences and the weak BN spots itself had a positive influence on crack deflection at the layer interfaces. The BN spots remarkably deflected or entrapped the propagating crack, as it is shown in Figs. 6a and b and increased the fracture toughness of layered composite.

The fracture toughness of layered L4B1 material was markedly higher (9.75 MPa $m^{1/2}$) in comparison to "monolithic" β-SiAlON + TiN sample, MB1 (4.71 MPa $m^{1/2}$) (Fig. 7). Because the TiN particles are present in both materials and so the crack deflection due to their presence is similar, the high increase of fracture toughness can be explained by the laminated structure and the reasonable thermal expansion mismatch between Si_3N_4 and SiAlON + TiN layers. The layer sequence with increasing amount of elongated β-Si_3N_4 seed particles, which induced gradual increase of compressive stress in the adjacent layers in this direction, and the elongated β-Si_3N_4 grains itself also contributed to the remarkable increase (107%) of fracture toughness. The fracture toughness is raised to some extent also by the thermal expansion mismatch stress between the grain boundary glass and Si_3N_4 or β-SiAlON grains.

The three point bending strength of sintered samples is shown in Fig. 8. Although, the monolithic MB1 sample was relatively weak (647 MPa), the strength of layered composites was much higher due to the presence of Si_3N_4 layers. The influence of reaction conditions on the final bending strength of layered materials is demonstrated on samples L4A1 and L4B1 in Fig. 8. Both samples have the same composition and layer sequence, but sample L4A1 has a lower strength due to the remaining porosity. The pores were not eliminated successfully in this sample due to the evolution of gaseous nitrogen [reaction Eq. (1)] during sintering. However, the good strength of L4A1 sample (1028 MPa) confirms the flaw tolerance of layered composite. This sample contained pores up to 50 μm in diameter,

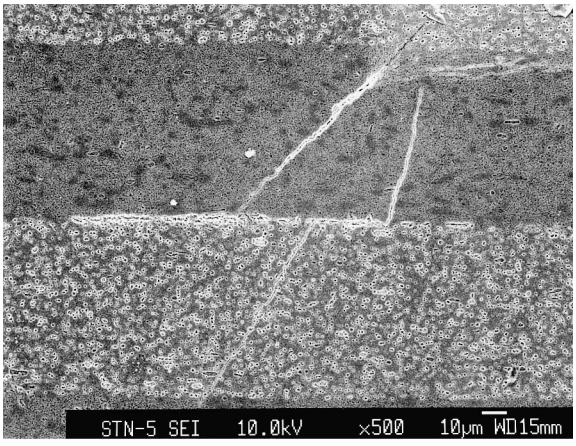

(a)

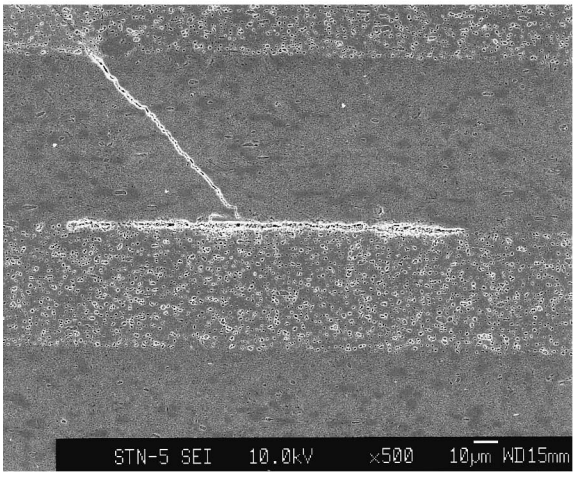

(b)

Fig. 6. Infuence of BN spots on the crack propagation: (a) crack deflection, (b) entrapped crack.

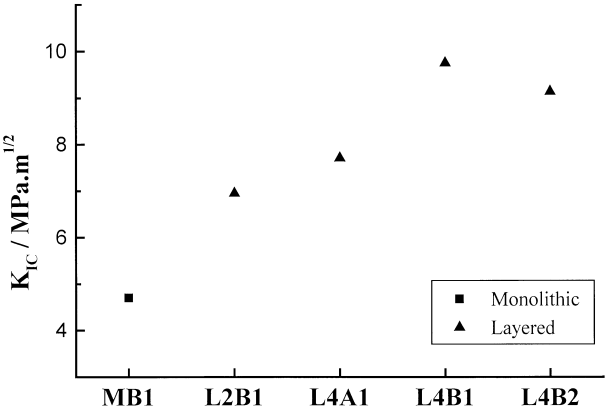

Fig. 7. Fracture toughness of monolithic and layered samples determined by SEVNB method.

however the critical flaw size calculated by the Griffith equation is only about 12 μm. The other samples, including the bulk MB1 sample with remarkably lower strength, were prepared under optimized conditions and were free of pores.

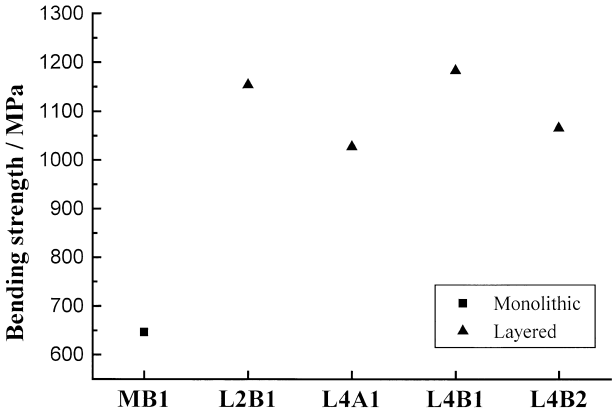

Fig. 8. Three-point bending strength of monolithic and layered samples.

The influence of layer sequence on strength is demonstrated on samples L2B1 and L4B1. However, there is no big difference in absolute values and the strength of both samples is more than 1150 MPa, the higher strength of L4B1 sample is most probably due to the higher volume fraction of Si_3N_4. The ratio of SN to SNT layers was 3:1 in L4B1 sample, while for the L2B1 sample it was only 1:1.

Samples L4B1 and L4B2 demonstrate the influence of TiN content. The strength of L4B2 sample with 20vol% TiN is lower in comparison to L4B1 sample (10% TiN); however, usually, for the particle reinforced Si_3N_4/TiN composites with increasing TiN content ($<40\%$) also the strength increases.[10] Because remaining porosity was not observed in these samples, the difference should be due to the higher tensile stress in the L4B2 sample (20% TiN) in comparison to L4B1 sample (10% TiN).

Comparing all samples, the L4B1 layered material has the highest strength and fracture toughness. In the case of mechanical properties it can be concluded that for the presented layer composition both the B heat treatment schedule and 10 vol% TiN are close to the optimum value.

3.3. Physical properties

The measured thermal conductivity and electrical resistivity of monolithic MB1 sample and layered L4B1, L4B2 with 10 and 20% TiN, respectively are listed in Tables 2 and 3. The tabulated values of monolithic materials are shown in Table 4 for a comparison.

As many properties, also the thermal and electrical conductivity are dependent on the composition of the material. For β-SiAlONs both properties are decreasing with increasing z value.[27,28] The chemical composition of β-SiAlON was measured on powdered MB1 sample with the help of X-ray unit cell determination. The calculated z values of β-SiAlON on the base of unit cell dimensions are $z=1.63$ and 3.81, which are in good agreement with the theoretical $z=1.71$ and 3.90 respectively, calculated from the starting composition. The published thermal conductivities of β-SiAlONs with close composition are 5.03 $Wm^{-1}\,K^{-1}$ ($z=1.44$) and 4.46 $Wm^{-1}\,K^{-1}$ ($z=4.04$),[28] which suggest that this component is responsible for low thermal conductivity of bulk SiAlON + 10 vol% TiN sample (MB1, Table 2). The theoretical estimation of thermal conductivity of layered composite is difficult due to the big scatter of published data for both TiN and Si_3N_4 (Table 4).

Anisotropic thermal conductivity was obtained for the layered material due to the lower thermal conductivity of (β-SiALON + TiN) layer in comparison to Si_3N_4 with elongated seed particles. The biggest anisotropy was obtained for the L4B2 sample. Although, generally for these layered samples in the case of thermal conductivity the differences in parallel and perpendicular direction are not so remarkable, because of smaller differences in this property for the monolithic materials (Table 4). It should be mentioned that the used material design offers to produce also Si_3N_4 based materials with high thermal conductivity (>60 $Wm^{-1}\,K^{-1}$), but they must be prepared with special care

Table 2
Thermal conductivity κ of monolithic (MB1) and layered samples (L4B1,2)[a]

Sample	κ_x	κ_y
	(W/mK)	(W/mK)
MB1	11.4	11.0
L4B1	19.5	10.7
L4B2	18.6	9.8

[a] Indices x and y indicate the parallel and perpendicular direction to the larger alignment.

Table 3
Electrical resistivity a of monolithic (MB1) and layered samples (L4B1,2)[a]

Sample	a_x (Ω cm)	a_y (Ω cm)
MB1	5×10^{6}	5×10^{6}
L4B1	8×10^{7}	2×10^{12}
L4B2	6×10^{-2}	5×10^{11}

Table 4
Tabulated values of electrical resistivity a and thermal conductivity κ of ceramic materials

Sample	a	κ
	(Ω cm)	(W/mK)
Si_3N_4	10^{13}	20–150
TiN	3×10^{-5}	24–50
β-SiAlON	10^{7}	2–6

(low content of oxide sintering additives, highly oriented coarse microstructure, etc.[29,30]), what was not the goal of this study. Lower thermal conductivity of L4B2 sample in comparison to L4B1 sample is most probably due to the higher internal stresses, which can generate more dislocations in the grains, and higher z value of β-SiAlON. As it was mentioned, the higher the z value, the lower the thermal conductivity; however, the differences are small (1–2 $Wm^{-1}K^{-1}$) and so it should not have remarkable influence. On the other hand, according to the higher volume content of TiN in L4B2 sample its thermal conductivity should be higher. These results indicate that the influence of residual stresses and the higher z value of the β-SiAlON are dominant over the increased TiN content.

Strong anisotropy in electrical conductivity was measured for the layered L4B2 sample with 20 vol% TiN in parallel (x) and perpendicular (y) direction to the layers. In parallel direction the electroconductive TiN increased the conductivity. However, though the TiN content was only 20 vol% in the (β-SiAlON + TiN) layer, good electrical conductivity was obtained for this layer due to the network-like distribution of TiN. The critical volumetric fraction calculated on the base of percolation theory for conductance is 20.9 vol%,[31] if the particles dispersed in the insulating matrix are connected. This may also suggest that the in situ formed TiN particles are in contact. The electrical conductivity of layered material was much lower in perpendicular direction to the layers, because the Si_3N_4 interlayers are insulators.

4. Conclusions

The reaction conditions for in situ preparation of β-SiAlON + TiN composite were optimized and pore-free ceramic material was prepared. Consequently dense Si_3N_4/(β-SiALON + TiN) layered composites were prepared under the same reaction conditions by hot pressing. The bending strength and fracture toughness of layered materials were remarkably higher (by 82 and 107%, respectively) in comparison to the conventional β-SiAlON + TiN composite. Anisotropic electrical and thermal properties were obtained for the layered materials, as it was designed and expected. The experimental results confirmed that the layered material design is suitable for the preparation of multifunctional ceramic materials.

Acknowledgements

Work was supported by NEDO as a part of Synergy Ceramics Project under the Industrial Science and Technology Frontier Program promoted by AIST, MITI, Japan. Part of the work was also supported by the Slovak Grant Agency VEGA, contract No. 2/5118/98. Appreciation is expressed to Dr. Karol Fröhlich for the measurement of electrical conductivity.

References

1. Harmer, M. P., Chan, H. M. and Miller, G. A., Unique opportunities for microstructural engineering with duplex and laminar ceramic composites. *J. Am. Ceram. Soc.*, 1992, **75**, 1715–1728.
2. Marshall, D. B., Ratto, J. J. and Lange, F. F., Enhanced fracture toughness in layered microcomposites of Ce-ZrO2 and Al_2O_3. *J. Am. Ceram. Soc.*, 1991, **74**, 2979–2987.
3. Chartier, T., Merle, D. and Besson, J. L., Laminar ceramic composites. *J. Eur. Ceram. Soc.*, 1995, **15**, 101–107.
4. Šajgalík, P., Lenčéš, Z. and Dusza, J., Si_3N_4 based composite with layered microstructure. In *5th Int. Symp. Ceramic Materials and Composites for Engines*, ed. D. S. Yan, X. R. Fu and S. X. Shi. World Scientific, Singapore/New Jersey/London/Hong Kong, 1995, pp. 198–201.
5. Šajgalík, P., Lenčéš, Z. and Dusza, J., Residual stresses in layered silicon nitride-based composites. In *Engineering Ceramics'96: Higher Reliability through Processing*. NATO ASI Series, 3. High Technology, Vol. 25. Kluwer Academic Publishers, Dordrecht/Boston/London, 1997, pp. 301-309.
6. Jack, K. H., Review: SiAlON and related nitrogen ceramics. *J. Mater. Sci.*, 1976, **11**, 1135–1158.
7. Gogotsi, Yu.G., Review: Particulate silicon nitride-based composites. *J. Mater. Sci.*, 1994, **29**, 2541–2556.
8. Yasutomi, Y. and Sobue, M., Development of reaction-bonded electroconductive TiN–Si_3N_4 and resistive Al_2O_3–Si_3N_4 composites. *Ceram. Eng. Sci. Proc.*, 1990, **11**(7–8), 857–867.
9. Yasutomi, Y., Chiba, A. and Sobue, M., Development of reaction–bonded electroconductive silicon nitride–titanium nitride and resistive silicon nitride–aluminum oxide composites. *J. Amer. Ceram. Soc.*, 1991, **74**(5), 950–957.
10. Bellosi, A., Guicciardi, S. and Tampieri, A., Development and characterization of electroconductive Si_3N_4–TiN composites. *J. Eur. Ceram. Soc.*, 1992, **9**, 83–93.
11. Lin, W., Yang, J. M., Ting, S. J., Ezis, A. and Shih, C. J., Processing and microstructural development of in situ TiN–reinforced silicon nitride/silicon oxynitride composites. *J. Am. Ceram. Soc.*, 1992, **75**(11), 2945–2952.
12. Huang, J. L., Lee, M. T., Lu, H. H. and Lii, D. F., Microstructure, fracture behaviour and mechanical properties of TiN/Si_3N_4 composites. *Mater. Chem. Physics*, 1996, **45**, 203–210.
13. Nagaoka, T., Yasuoka, M., Hirao, K. and Kanzaki, S., Effects of TiN particle size on mechanical properties of Si_3N_4/TiN particulate composites. *J. Ceram. Soc. Japan, Int. Ed.*, 1992, **100**, 612–614.
14. Sato, Y. and Ueki, M., Processing and mechanical properties of Si_3N_4–SiC whisker–TiN system composite materials. *J. Ceram. Soc. Japan, Int. Ed.*, 1993, **101**, 354–357.
15. Crampon, J. and Duclos, R., Creep and microstructure of electrical dischrage machinable Si_3N_4 composites. *Acta Metall. Mater.*, 1990, **38**(5), 805–810.
16. Hillinger, G. and Hlavacek, V., Direct synthesis and sintering of silicon nitride/titanium nitride composite. *J. Am. Ceram. Soc.*, 1995, **78**(2), 495–496.
17. Shih, C. J., Yang, J. M. and Ezis, A., Feasibility study of developing an in situ TiN–reinforced Si_3N_4 composite. *Scr. Metall.*, 1990, **24**, 24119–241124.
18. Hong, F., Lumby, R. J. and Lewis, M. H., TiN/Sialon composites via in-situ reaction sintering. *J. Eur. Ceram. Soc.*, 1993, **11**, 237–239.
19. Ekström, T., SiAlON composite materials. In *Proceedings of the International Conference on Silicon Nitride-Based Ceramics*. In

Key Eng. Mater., ed. M. J. Hoffmann, P. F. Becher and G. Petzow. Trans Tech Publications, Aedermannsdorf, 1994, pp. 327–332.
20. Lenčéš, Z., Preparation of Si_3N_4-based materials. PhD thesis, Slovak Technical University, Bratislava, Slovakia, 1996.
21. Huang, J. L., Chou, F. C. and Lu, H. H., Investigation of Si_3N_4–TiN/Si_3N_4–Si_3N_4 trilayer composites with residual surface compression. *J. Mater. Res.*, 1997, **12**(9), 2357–2365.
22. Šajgalík, P. and Lenčéš, Z., Microstructurally induced internal stresses in the silicon nitride layered composites. In *Ceramic Microstructure: Control at the Atomic Level*, ed. A. P. Tomsia and A. Glaeser. Plenum Press, New York, 1998, pp. 795–802.
23. Hirao, K., Tsuge, A., Brito, M. E. and Kanzaki, S., Preparation of rod-like β-Si_3N_4 single crystal particles. *J. Ceram. Soc. Japan*, 1993, **101**(9), 1078–1080.
24. Šajgalík, P., Lenčéš, Z. and Dusza, J., Layered Si_3N_4 composites with enhanced room temperature properties. *J. Mater Sci.*, 1996, **31**, 4837–4842.
25. Šajgalík, P. and Lenčéš, Z., Silicon nitride layered composites — relationship between residual stresses and fracture behaviour. In *Ceramic Materials and Components for Engines*, ed. K. Niihara et al. Technoplaza Co, Japan, 1998, pp. 675–678.
26. Messier, D. R. and Croft, W. J., Silicon nitride. In *Preparation and Properties of Solid State Materials, Vol. 7*, ed. W. R. Wilcox. Marcel Dekker Inc, New York/Basel, 1982, pp. 178–179.
27. Gauckler, L. J., Prietzel, S., Bodemer, G. and Petzow, G., Some properties of β-$Si_{6-x}Al_xO_xN_{8-x}$. In *Nitrogen Ceramics*, ed. F. L. Riley. Riley, Noordhoff Int. Publ, The Netherlands, 1977, pp. 529–537.
28. Haviar, M., Shneider, J., Kubičár, L., Boháč, V., Melandri, C., Guicciardi, S., Dusza, J. and Rudnayova, E., Physical properties of yttrium α- and β-SiAlONs. *J. Eur. Ceram. Soc.*, Submitted for publication.
29. Watari, K., Hirao, K., Brito, M.E., Toriyama, M. and Kanzaki, S., Hot-isostatic-pressing to increase thermal conductivity of Si_3N_4 ceramics. *J. Mater. Res.*, 1999, **14**(14), 1538–1541.
30. Hirosaki, N., Ando, M., Okamoto, Y., Munakata, F., Akimune, Y., Hirao, K., Watari, K., Brito, M. E., Toriyama, M. and Kanzaki, S., Effect of alignment of large grains on the thermal conductivity of self-reinforced β-silicon nitride. *J. Ceram. Soc. Japan Int. Ed.*, 1997, **104**, 1187–1190.
31. Dean, P. and Bird, N.F., Math Divisional Rep., May 61 of the National Physical Lab., Teddington, UK. 1966.